PHYSICAL REVIEW B **79**, 201306(R) (2009)

Ultrafast nonlinear optical response of photoexcited Ge/SiGe quantum wells: Evidence for a femtosecond transient population inversion

C. Lange,[1,*] N. S. Köster,[1] S. Chatterjee,[1] H. Sigg,[2] D. Chrastina,[3] G. Isella,[3] H. von Känel,[3] M. Schäfer,[4] M. Kira,[4] and S. W. Koch[4]

[1]*Faculty of Physics and Material Sciences Center, Philipps-Universität, Renthof 5, D-35032 Marburg, Germany*

[2]*Laboratory for Micro and Nanotechnology, Paul Scherrer Institut, CH-5232 Villigen PSI, Switzerland*

[3]*Dipartimento di Fisica del Politecnico di Milano, CNISM and L-NESS, Polo di Como, via Anzani 42, I-22100 Como, Italy*

[4]*Department of Physics and Material Sciences Center, Philipps University, Renthof 5, D-35032 Marburg, Germany*

(Received 4 March 2009; revised manuscript received 28 April 2009; published 19 May 2009)

Femtosecond time-resolved pump-probe spectroscopy is used to investigate the ultrafast carrier dynamics of Ge/SiGe quantum wells grown on a Si substrate. Pronounced nonequilibrium effects in the relaxation dynamics of the optically injected carrier distributions are observed and analyzed using a microscopic many-body theory. Transient population inversion and optical gain is obtained on a femtosecond time scale for excitation at energies slightly above the lowest direct quantum-well transition.

DOI: 10.1103/PhysRevB.79.201306 PACS number(s): 78.67.De, 78.40.Fy, 78.47.Fg, 78.47.J−

The optical properties of direct-gap *III-V* semiconductor materials and their heterostructures have been the subject of intense investigations over the last several decades.[1–4] Model systems with direct optical band gaps, such as GaAs/(AlGA)As quantum wells (QWs), have been thoroughly investigated down to the ultrafast fs time regime, revealing their nonequilibrium properties.[1,3]

More recently, the ultrafast response of heterostructures based on materials with indirect band gap, most prominently Si and Ge, has attracted great attention. The observation of the quantum confined Stark effect,[5,6] interband absorption,[7,8] and emission[9] in SiGe systems is unambiguously attributed to optical transitions at the Γ-point.[6] Thus, even in indirect band gap semiconductors such as Ge/SiGe QWs, the optical properties are governed by electronic states in the vicinity of the center of the Brillouin zone. In this Rapid Communication, we investigate the ultrafast carrier dynamics and the resulting nonequilibrium response of strained Ge/SiGe QWs grown on a Si substrate.

The sample consists of 50 compressively strained Ge QWs which were grown by low-energy plasma-enhanced chemical vapor deposition (LEPECVD) (Ref. 10) on a (001)-oriented silicon substrate. The 14-nm-wide QWs are separated by 20-nm-thick $Si_{0.15}Ge_{0.85}$ barriers. The compressive (tensile) strain in the QW (barrier) layers is set by a relaxed SiGe buffer linearly graded from Si to $Si_{0.1}Ge_{0.9}$. In the QWs, the strain breaks the degeneracy of heavy-hole (hh) and light-hole (lh) states in the valence band. The electronic structure of a similar sample has been investigated in detail by means of tight-binding calculations[6] and transmission spectroscopy[9] from which the fundamental optical transitions between the electronic states can be identified. The linear absorption spectrum for low temperature (10 K) is plotted in the bottom part of Fig. 1. The fundamental direct transitions between hh and lh states to the conduction-band states at the Γ point ($c\Gamma$) all show a distinct excitonic enhancement, which is most pronounced for the hh-related transitions. The clear steplike shape of the absorption exhibits low inhomogeneous broadening of 6 meV for the lowest-lying transition hh1-$c\Gamma$1. Both are indications of the high structural quality of the sample, as confirmed independently by high-resolution x-ray diffraction measurements.[11] The indirect, phonon-assisted transition to the global minimum of the conduction band is not visible in the linear absorption spectrum. Experi-

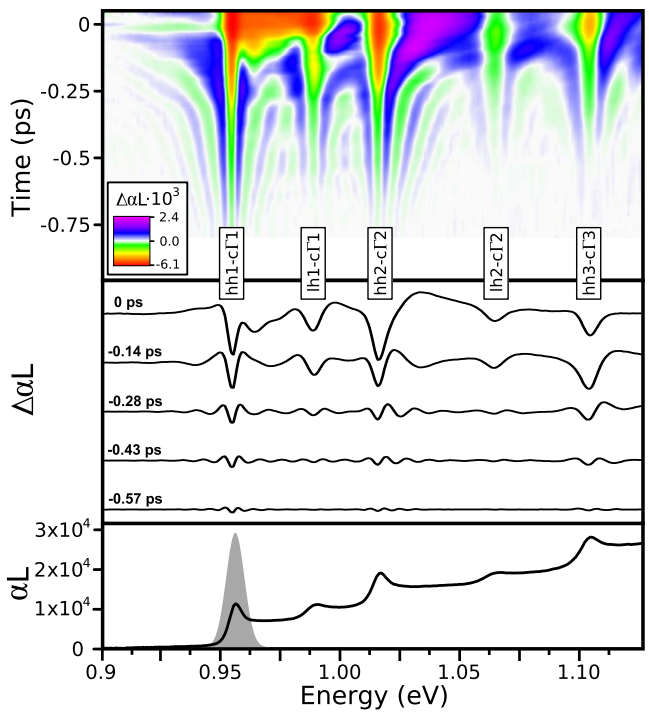

FIG. 1. (Color online) Low-temperature absorption spectra at 10 K. Top: differential absorption for $t<0$ in false-color coding for excitation at 0.955 eV (gray pulse shape). Neighboring lines in green and blue (gray lines separated by white lines) indicate coherent oscillations of the polarization, diverging in wavelength as $t=0$ is approached. Center: selected spectra (horizontal cuts) for different times reveal the symmetric and antisymmetric shapes of the oscillations for transitions resonant (hh1-$c\Gamma$1) and nonresonant (hh2-$c\Gamma$2, hh3-$c\Gamma$3) to the pump, respectively. Bottom: linear absorption spectrum.

ments show that it is located about 140 meV below the hh1-$c\Gamma 1$ transition at 293 K.[9]

We perform ultrafast pump-probe experiments using strong, 80-fs-long pump pulses from an optical parametric amplifier (OPA) and spectrally broad probe pulses from a white-light supercontinuum source. Both are driven by a regenerative 1 kHz Ti:sapphire amplifier. The OPA allows for a continuous tuning of the excitation energy, while the broadened supercontinuum enables us to monitor the full spectral range of interest. The experimental setup yields sub-50 fs temporal resolution. The sample was mounted under Brewster's angle to minimize reflection losses. Changes in the residual reflection are found to be negligible as verified in a separate pump-probe experiment. Monitoring the transmission, the experiment thus yields differential absorption spectra according to Beer's law, rendering the pump-induced change in absorption as a function of energy and time.

In our first set of experiments, we excite the sample resonantly at the hh1-$c\Gamma 1$ transition at a lattice temperature of 10 K. The resulting differential absorption spectra are shown in the top part of Fig. 1 plotted in false colors; the excitation is indicated by the gray pulse shape. The spectra are shown from 750 fs before the excitation up to the time zero and are acquired with a step size of 30 fs. Initially, the absorption remains unchanged (white).

As the time zero is approached, coherent oscillations of the polarization become visible as neighboring lines shown in blue and green (gray lines separated by white lines). The spectral oscillation period ultimately diverges toward time zero.[12] Thus, the coherent oscillations act as an internal clock; the temporal overlap of pump and probe pulse can be calibrated elegantly by this intrinsic response of the electronic system. Around time zero, the absorption is heavily bleached (yellow and reddish color) as large amounts of carriers are created and further excitations become less likely. The spectra shown in the center part of Fig. 1 are horizontal cuts at five different time delays: 0.57, 0.43, 0.28, and 0.14 ps before excitation and at time zero (from bottom to top). They show the coherent oscillations in more detail: the shape is symmetrical for transitions resonant to the excitation, i.e., at the hh1-$c\Gamma 1$-transition, but dispersive and antisymmetric for energies nonresonant to the pump, such as for hh2-$c\Gamma 2$ and hh3-$c\Gamma 3$, in accordance with Ref. 12.

Second, we investigate the scattering dynamics at room temperature when exciting the sample at the hh3-$c\Gamma 3$ transition. Typical results are summarized in Fig. 2 showing four differential absorption spectra at positive time delays. The differential absorption spectrum at 1 ps after excitation is plotted as a reference (dotted gray line). At this time, the system has reached a quasiequilibrium state. The absorption is most heavily bleached at the injection energy at 0 ps. Subsequently, the carriers scatter toward lower energies via deformation potential scattering, as can be observed by the shift of the center of bleaching signature.

Most of the carriers occupy states in the vicinity of the hh2-$c\Gamma 2$ transition after about 250 fs, further moving toward lower energy after about 450 fs. Eventually, the holes occupy the first heavy-hole state only. The electrons are quickly moved to the L states by intervalley phonon scattering. The spectral shape of the differential absorption in this quasiequilibrium state is governed by charge screening.[3] The quasiequilibrium state remains unchanged for more than 1 ns. This is in good agreement with typical lifetimes observed in high-quality Ge that may even extend into the μs regime.[13] In total, a nonequilibrium carrier distribution and its thermalization are observed over a time scale of 500 fs for a moderate carrier density of 10^{11} cm^{-2}. It should be noted that such relaxation processes are significantly faster in typical *III-V* materials where phonon scattering times in the range of 100 fs are found,[14,15] driven by the more efficient Fröhlich interaction. Here, the slow intravalley relaxation can thus be attributed to the lack of Fröhlich interaction since the crystal bonds are purely covalent. Furthermore, deformation potential scattering is comparatively less efficient for scattering processes with small momentum transfer. Therefore, the Γ-to-L depopulation is more efficient here than the intravalley cooling.

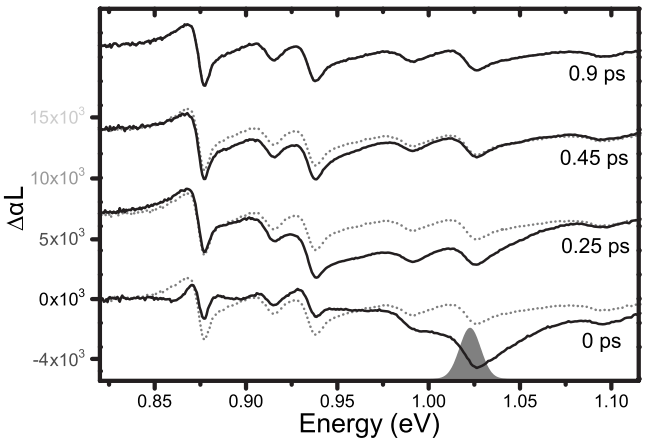

FIG. 2. Nonthermal carrier distribution at 293 K after nonresonant excitation at 1.02 eV (gray pulse shape). Four differential absorption spectra show the relaxation toward the quasi-steady-state at 1 ps, plotted in gray for reference. As time increases (bottom to top), carriers scatter toward lower energy, causing the center of bleaching to follow.

In a third set of experiments, we investigate the sample response at room temperature under high-power excitation. When the sample is pumped slightly above the hh1-$c\Gamma 1$ transition, we find at early times a high-density electron population energetically close to the pump energy. As the carriers relax, we observe ultrafast transient gain at the direct energy gap of the Ge QWs indicating carrier population inversion around the Γ point. Examples of the results are shown in Fig. 3 for an excitation at 0.91 eV in the continuum of the hh1-$c\Gamma 1$ transition at a pump photon density of 2.5×10^{19} cm^{-2} per pulse. We see in Fig. 3(a) that a peak gain of $\alpha L=-8\times 10^{-4}$ per QW is reached. The gain lasts for about 20 fs. The photon flux applied here is about 3 orders of magnitude larger than that needed to drive a direct-gap *III-V* semiconductor into the gain regime under comparable excitation conditions.[16] Decreasing the pump intensity at the same energy to one-third in another experiment yields a maximum gain value of $\alpha L=-2.5\times 10^{-4}$ (not shown here). Due to the slower scattering processes, gain was achieved for 60 fs in the latter case.

Our measurements show that significantly reduced or no

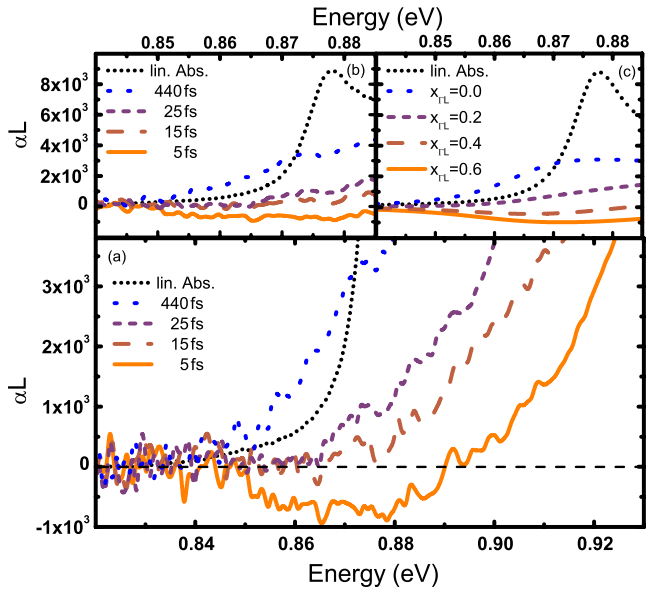

FIG. 3. (Color online) Absorption spectra around the hh1-$c\Gamma 1$ transition at 293 K. [(a) and (b)] Experimental absorption spectra for 5, 15, 25, and 440 fs (bottom to top) after the excitation. Maximum gain value of $\alpha L = 8 \times 10^{-4}$ per QW is found. (c) Corresponding theoretical spectra are selected by line-shape comparison and plotted as a function of $x_{\Gamma L} = n_{e\Gamma}/n_e$ with values of 0.6, 0.4, 0.2, and 0 (bottom to top), following the decay of the Γ-point population. The linear absorption spectrum is plotted as a black dotted line for reference.

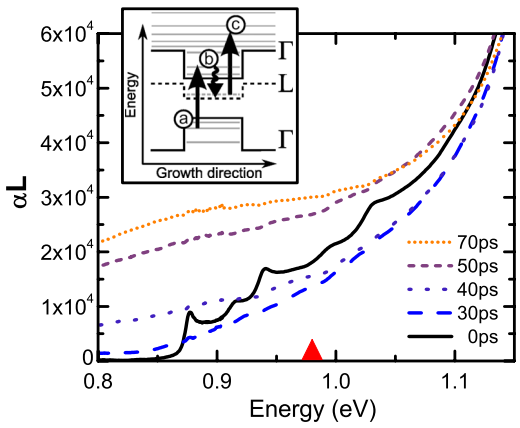

FIG. 4. (Color online) Absorption spectra for quasi-cw excitation at 293 K. The black solid line represents the linear absorption spectrum. The broken lines show the absorption of 30, 40, 50, and 70 ps (from bottom to top) after excitation at 0.98 eV (red/gray pulse shape). The emerging absorption is attributed to L-state absorption, as schematically depicted in the inset. Carriers are excited (a) into the Γ valley of the conduction band, from where they quickly scatter (b) into the L valley. From there, they are further excited (c) into higher states above the barrier.

gain at all is observed when the sample is excited at energies above 0.91 eV. In these cases, the electrons undergo a series of scattering events via intermediate states which allow them to scatter to the L valley before ever reaching the $c\Gamma 1$ state. Therefore, fewer and fewer carriers contribute to population at the direct transition as the injection is moved toward higher energies.

We perform a theoretical analysis based on a microscopic theory in order to analyze the excitation kinetics in more detail. Our approach is based on the semiconductor Bloch equations[3] which render the susceptibility as a function of carrier density and material parameters. Coulomb interaction and thus particle scattering is treated via the systematic cluster-expansion technique.[17] The particle correlations are split into a factorized single-particle contribution according to Hartree-Fock and a series of interaction terms, accounting for the scattering mechanisms of the carrier system. The expansion is truncated at the level of two-particle correlations as no further improvement is obtained by including higher orders. The numerical evaluation yields absorption spectra for different excitation conditions.

The electron density n_e is split into the two fractions residing in the L and Γ valleys to account for the indirect conduction-band structure: $n_e = n_{e\Gamma} + n_{eL}$. The holes are assumed to stay in the hh1 level; note that the hole density n_h is equal to the total electron density n_e. All subbands are populated according to their respective Fermi functions at a lattice temperature of 293 K at $t=0$ fs. The electron density n_e and conduction-band population ratio $x_{\Gamma L} = n_{e\Gamma}/n_e$ are determined by comparing experimental and theoretical absorption line shapes. An example is shown in Figs. 3(b) and 3(c), where spectra are plotted from the point of maximum gain onwards. An electron density of $n_e = 1.7 \times 10^{12}$ cm^{-2} ($n_e = 7.5 \times 10^{11}$ cm^{-2} for excitation with less power) is obtained for a series of values for $x_{\Gamma L}$. Due to scattering to the L valley which is immediately effective, the ratio $x_{\Gamma L}$ does not reach unity.

The exponential decay rate τ is found to be 20 and 110 fs for the high- and low-density cases, respectively. Transparency is reached at the Γ point for an electron density of about 4.7×10^{11} cm^{-2}, corresponding to $x_{\Gamma L} = 0.3$ and $x_{\Gamma L} = 0.6$, respectively. Comparing both cases, the inverse quadratic dependence $\tau \propto n^{-2}$ is observed. This relation indicates the importance of electron-electron scattering which assists the Γ-to-L intervalley transfer scattering.

The reason for the short gain lifetime in this material is the strong carrier drainage effect of the L valley. Both strain engineering to shift the L states upwards in energy and filling them up by doping have been discussed.[18] Here, we follow the latter approach by optically generating a very large carrier density. This is accomplished by stretching the pump pulse to 80 ps, reducing the effects of Rabi oscillations and Pauli blocking. The sample is held at room temperature and excited at 0.98 eV. Significantly more carriers are generated even for almost an order of magnitude smaller photon flux (10^{18} cm^{-2} per pulse). The corresponding experimental data are plotted in Fig. 4, where absorption spectra from 0 to 70 ps after the excitation are shown along with the linear absorption spectrum. A massive increase in the overall absorption, extending into the spectral region below the direct band gap, is observed. It originates from the high electron density created in the L states of the conduction band. These free carriers absorb light and are excited into a multitude of higher states of the band structure. The spectral shape of this additional absorption channel is flat and featureless.[19] In a

separate experiment (not shown here), the *L*-state absorption is monitored below the band gap as a function of temperature. We find that the absorption magnitude scales logarithmically with temperature, indicating a phonon-assisted mechanism.

The broadband *L*-state absorption is equivalent to, but much stronger than free carrier absorption, a loss channel in semiconductor lasers.[20] We expect that creating a large density of free carriers, e.g., by doping, will increase the overall absorption to a larger extent than it facilitates achieving gain.

In conclusion, we have investigated the nonequilibrium ultrafast response of Ge/SiGe QWs, a model system for indirect-gap semiconductor quantum-well materials. Carrier thermalization, relaxation, and intravalley scattering are observed; and the characteristic times are identified. Transient optical gain is obtained for strong optical interband excitation slightly above the energetically lowest exciton resonance. The required Γ-point population inversion results from the temporal mismatch between the relatively fast intraband relaxation of the optically generated conduction-band electrons and the rather slow intravalley carrier-phonon scattering under these excitation conditions.

We thank W. W. Rühle for helpful and constructive discussions. We acknowledge financial support by the Deutsche Forschungsgemeinschaft, the Swiss Science Foundation, and the CARIPLO project SIMBAD.

*christoph.lange@physik.uni-marburg.de

[1] Jagdeep Shah, in *Ultrafast Spectroscopy of Semiconductors and Semiconductor Nanostructures*, 2nd ed. (Springer-Verlag, Berlin, 1999).

[2] Claus F. Klingshirn, in *Semiconductor Optics*, 3rd ed. (Springer-Verlag, Berlin, 2006).

[3] H. Haug and S. W. Koch, *Quantum Theory of the Optical and Electronic Properties of Semiconductors*, 5th ed. (World Scientific, Singapore, 2009).

[4] W. Schäfer and M. Wegener, *Semiconductor Optics and Transport Phenomena* (Springer-Verlag, Berlin, 2002).

[5] Y. H. Kuo, Y. K. Lee, Y. Ge, S. Ren, J. E. Roth, T. I. Kamins, D. A. B. Miller, and J. S. Harris, Nature (London) **437**, 1334 (2005).

[6] M. Virgilio and G. Grosso, J. Phys.: Condens. Matter **18**, 1021 (2006).

[7] M. Virgilio, M. Bonfanti, D. Chrastina, A. Neels, G. Isella, E. Grilli, M. Guzzi, G. Grosso, H. Sigg, and H. von Känel, Phys. Rev. B **79**, 075323 (2009).

[8] S. Tsujino, H. Sigg, D. Chrastina, and H. von Känel, Appl. Phys. Lett. **89**, 262119 (2006).

[9] M. Bonfanti, E. Grilli, M. Guzzi, M. Virgilio, G. Grosso, D. Chrastina, G. Isella, H. von Känel, and A. Neels, Phys. Rev. B **78**, 041407(R) (2008).

[10] B. Rössner, D. Chrastina, G. Isella, and H. von Känel, Appl. Phys. Lett. **84**, 3058 (2004).

[11] D. Chrastina, A. Neels, M. Bonfanti, M. Virgilio, G. Isella, E. Grilli, M. Guzzi, G. Grosso, H. Sigg, and H. von Känel, *Proceedings of the IEEE Fifth International Conference on Group IV Photonics* (IEEE, 2008), p. 194.

[12] S. W. Koch, N. Peyghambarian, and M. Lindberg, J. Phys. C **21**, 5229 (1988).

[13] R. N. Hall, Phys. Rev. **87**, 387 (1952).

[14] M. U. Wehner, M. H. Ulm, D. S. Chemla, and M. Wegener, Phys. Rev. Lett. **80**, 1992 (1998).

[15] Q. T. Vu, H. Haug, W. A. Hügel, S. Chatterjee, and M. Wegener, Phys. Rev. Lett. **85**, 3508 (2000).

[16] C. Lange, S. Chatterjee, C. Schlichenmaier, A. Thränhardt, S. W. Koch, W. W. Rühle, J. Hader, J. V. Moloney, G. Khitrova, and H. M. Gibbs, Appl. Phys. Lett. **90**, 251102 (2007).

[17] J. Fricke, Ann. Phys. **252**, 479 (1996).

[18] J. Liu, X. Sun, D. Pan, X. Wang, L. C. Kimerling, T. L. Koch, and J. Michel, Opt. Express **15**, 11272 (2007).

[19] W. P. Dumke, M. R. Lorenz, and G. D. Pettit, Phys. Rev. B **1**, 4668 (1970).

[20] A. Haug, Semicond. Sci. Technol. **7**, 373 (1992).